AEROSOL TYPES AND CHARACTERISTICS MEASURED WITH AIRBORNE LIDAR DURING INTEX-NA

Carolyn F. Butler[(1)], Edward V. Browell[(2)] , Richard A. Ferrare[(2)], Johnathan W. Hair[(2)], Syed Ismail[(2)], Vincent G. Brackett[(1)], Marta A. Fenn[(1)], Anthony Notari[(1)], Susan A. Kooi[(1)] and Sharon P. Burton[(1)]

[(1)] *SAIC/NASA Langley Research Center, MS 929, Hampton, VA 23681, USA*
Email: c.f.butler@larc.nasa.gov, v.g.brackett@larc.nasa.gov,m.a.fenn@larc.nasa.gov ,a.notari@larc.nasa.gov, s.a.kooi@larc.nasa.gov, s.p.burton@larc.nasa.gov
[(2)]*NASA Langley Research Center, Hampton, VA, MS 401A, Hampton, VA 23681, USA,*
Email: e.v.browell@larc.nasa.gov,r.ferrare@larc.nasa.gov, j.w.hair@larc.nasa.gov, s.ismail@larc.nasa.gov

ABSTRACT

The NASA Langley Research Center Differential Absorption Lidar (LaRC/DIAL) system has participated in many airborne global tropospheric and stratospheric campaigns since 1980, collecting profiles of ozone (O_3) and aerosol distributions. For tropospheric campaigns, aerosol depolarization has been measured in the nadir since 1999 and simultaneously in both the nadir and zenith since 2004. The current configuration of this system was flown on the NASA DC-8 during the Intercontinental Chemical Transport Experiment - North America (INTEX-NA) conducted in the summer of 2004. The DIAL's remote profile measurements were made from near the surface to above the tropopause along the flight track of the DC-8. The DIAL system was used to determine the large-scale variability of air masses being sampled in situ on the DC-8 and to direct the in situ sampling strategy in real time. While the O_3 measurement has been an excellent tracer of both stratospheric air and of tropospheric pollution, aerosol depolarization is key to detecting smoke and dust plumes. During the summer of 2004, smoke plumes from Alaska were frequently observed with depolarizing aerosols over eastern North America. On two flights, highly depolarizing dust from the Sahara was observed over central regions of the US. This paper discusses the types and characteristics of aerosols that were encountered during this field experiment.

1. INSTRUMENTATION AND METHODOLOGY

The DIAL instrument has been described in detail in several recent publications [1, 2]. This system uses two 30-Hz, frequency-doubled Nd:YAG lasers to sequentially pump two dye lasers that are frequency-doubled into the UV. In the tropospheric configuration, the DIAL instrument transmits four wavelengths (1064, 576, 288.2, 299.6 nm) below and four wavelengths (1064, 599, 288.2, 299.6 nm) above the NASA DC-8 aircraft. The UV wavelengths are used for the DIAL measurement of ozone, while the two remaining wavelengths provide aerosol backscattering profiles in each direction. Additionally, a depolarization measurement is obtained by optically separating the 576 and 599 nm backscatter returns into parallel and perpendicular components.

The backscattered lidar return is adjusted for electronic and optical background; range squared; gain and energy normalized; and divided by a molecular density profile interpolated from the seasonal, latitudinal, and altitudinal tables of the Air Force Geophysical Lab [3]. These profiles are then normalized in a relatively clean region of the atmosphere. The aerosol scattering ratio (S), which is defined as the ratio of aerosol to molecular backscattering, is obtained by subtracting one from the normalized profiles. This is done for the 1064 nm returns (IR) and for the 576 and 599 nm returns (VS). S_{VS} profiles are corrected for molecular attenuation but neither wavelength is corrected for the unknown aerosol attenuation.

The wavelength dependence of the aerosol scattering ratios, S_{IR} and S_{VS}, can range from 0 to 4 representing very large to essentially molecular sized particles, respectively. The wavelength dependence is calculated from the relationship

$$\alpha = 4 - [\ln (S_{IR} / S_{VS}) / \ln (\lambda_{IR} / \lambda_{VS})] \quad (1)$$

where λ_{IR} = 1064 nm and λ_{VS} = 576 nm (nadir) and 599 nm (zenith). Due to the uncertainties in the normalization regions which may not be totally aerosol free, the aerosol wavelength dependence is only calculated if $S_{IR} > 0.3$ and $S_{VS} > 0.13$. The aerosol depolarization (δ_{aer}) is defined by

$$\delta_{aer} = [\delta_{tot} (S_{||} + 1) - \delta_{mol}] / S_{||} \quad (2)$$

where $S_{||}$ is the parallel component of S_{VS}, δ_{tot} is the total depolarization from both aerosols and molecules (the ratio of the perpendicular to the parallel lidar returns), and δ_{mol} is the molecular depolarization

calculated as 0.4%. The aerosol depolarization was calculated only when $S_{VS} > 0.17$.

2. AEROSOL TYPES AND CHARACTERISTICS

An air mass characterization scheme has been developed and used for previous tropospheric campaigns [2]. The ozone distribution, the S_{VS} and the potential vorticity are used to bin the air masses observed into various categories. This general categorization of the air masses was adapted for this with additional categories using the depolarization to discriminate between dust, biomass burning and other aerosol plumes. The results of this analysis are discussed in a companion presentation [4]. In a previous analysis, an attempt was made to average the aerosol characteristics within each air mass category for the TRACE-P campaign. However, the aerosol characteristics were often obscured by the broader scope of each category. This work addresses the types of aerosols observed during this campaign and the range of aerosol scattering ratio, depolarization and wavelength dependence for these types. Examples of these four aerosol products are shown in Fig. 1.

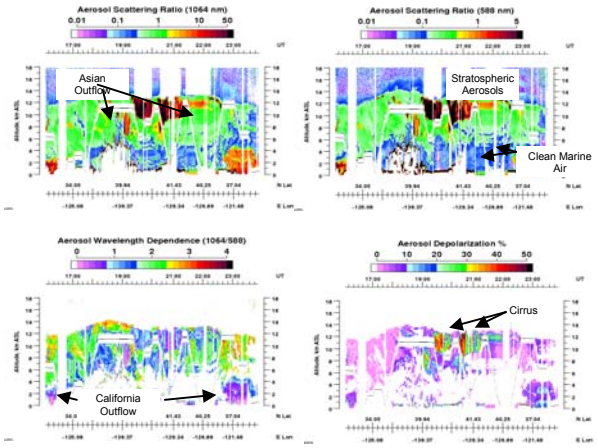

Fig. 1. DIAL aerosol products showing several aerosol types observed on flight off the coast of California on 1 July 2004. Top 2 panels are aerosol scattering ratios, bottom left is backscatter wavelength dependence and bottom right is aerosol depolarization.

2.1 Background aerosols

Out of the 17 science flights during INTEX-NA, only 6 flights were characterized by relatively clean aerosol loading above the boundary layer ($S_{IR} < 0.2$, $S_{VS} < 0.1$). These background aerosols were typically found in regions of convective activity and out over the Atlantic in the absence of continental outflow. These cleaner regions were also frequently observed above the enhanced aerosols in the free troposphere.

2.2 Free-tropospheric aerosols

Elevated aerosols were seen throughout the free troposphere on most flights over the North American continent accompanied by ozone levels from 50 to 75 ppbv, indicating probable pollution sources. These were typically smaller particles, $\alpha \sim 1.78$ with no depolarization, $\delta_{aer} < 0.4\%$, $S_{IR} \sim 0.51$ and $S_{VS} \sim 0.14$.

2.3 Boundary layer aerosols

Boundary layers aerosols, mainly from anthropogenic sources, but which might also include a mixture with dust and/or smoke, were characterized by high scattering ($1 < S_{IR} < 50$, $0.3 < S_{VS} < 2$), large particles ($\alpha < 1$), and no depolarization ($\delta_{aer} < 0.5\%$). These were observed persistently over the continental US and in the outflow off the continent over the mid-Atlantic, and, depending on the time of day, were confined below anywhere from 2 km (early morning) to 5 km (afternoon) above the surface.

2.4 Marine boundary layer

The marine boundary layers aerosols, mainly sea salts, were found below 1.5 km and were characterized by moderately high scattering ratios ($3 < S_{IR} < 15$, $0.2 < S_{VS} < 1$), large particles ($\alpha < 0.5$), and no depolarization ($\delta_{aer} < 0.5\%$). These aerosols were observed on the one flight over the Pacific (1 July) and on a few flights over the Atlantic.

2.3 Biomass burning

Long-range transport of fire plumes from Alaska was frequently observed with depolarizing aerosols over mid and eastern North America. Fig. 2 shows a highly scattering ($S_{IR} \sim 25$, $S_{VS} \sim 3$), optically thick plume encountered off the coast of Nova Scotia with moderate depolarization ($\delta_{aer} \sim 3.5\%$) and low wavelength dependence ($\alpha < 1$). Observations of Alaskan plumes on several other flights appeared as distinct ribbons of smoke from aerosols when above the boundary layer but mixed with anthropogenic aerosols within the boundary layer. Ozone was often photochemically produced within these layers. Very fresh smoke plumes from Arizona were also observed on flights out of St. Louis.

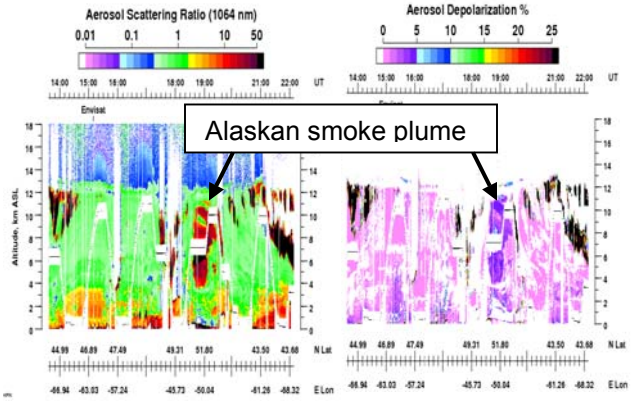

Fig. 2. Alaska smoke plume observed on 18 July 2004.

2.4 Dust

Although dust was only observed on two flights, it was easily distinguished by high depolarization (δ_{aer} ~ 12 - 20%) and large particles (α < 0.5 and S_{IR} ~ 8, S_{VS} ~ 0.7) (Fig. 3). The dust appeared to be mixed with other aerosols in the boundary layer. Back trajectories provided by the NOAA FLEXPART model suggest origins from the Sahara.

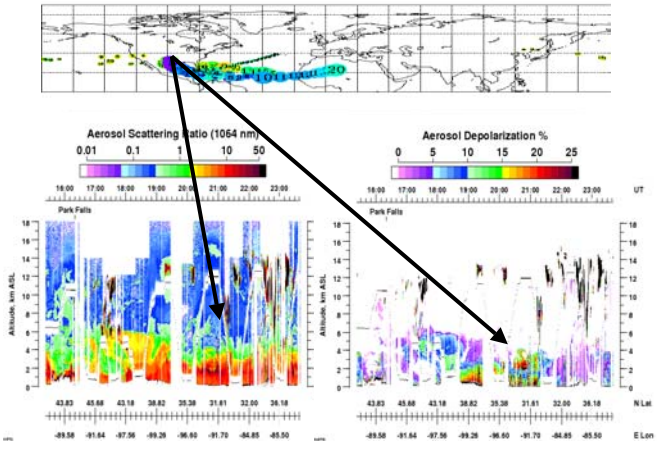

Fig. 3. Saharan dust observed over Oklahoma on 12 July 2004.

2.7 Aged Asian air

Asian pollution was observed on several flights with aerosols not necessarily unique in their characteristics but identifiable by enhancements over background aerosols in the upper troposphere. These air masses were usually mixed with stratospheric air containing very high O_3 ($0.5 < S_{IR} < 1$, $0.2 < S_{VS} < 0.5$, $\delta_{aer} < 1\%$, $1.5 < \alpha < 2.5$, O_3 ~ 60 to 180 ppbv).

2.8 Convective outflow

As with Asian pollution, these aerosols were not identifiable by their characteristics, but rather by enhancements over background aerosols in the upper troposphere and the presence of nearby clouds. These air masses were very similar in characteristics to aged Asian pollution (S_{IR} ~ 0.5 to 5, S_{VS} ~ 0.2 to 1, $\delta_{aer} < 1\%$, α ~ 1 to 2, O_3 ~ 70 to 170 ppbv). Note that convection over clean maritime regions could actually result in less aerosol and O_3 at upper altitudes than the surrounding regions, which has often been the case over clean regions of the Pacific.

2.9 Clouds

A wide range of clouds and cloud properties were observed throughout the troposphere. Near the tropopause, there were often cirrus with high scattering and depolarizations around 50% and sometimes sub-visible cirrus with much smaller scattering ratios and depolarizations. Near the surface, water clouds with no depolarization were often observed (although multiple scattering effects from these clouds generally gave the appearance of having depolarization).

3. SUMMARY

Many different types of aerosols were observed over North American during the summer of 2004. Aerosols (and O_3) were elevated in the free troposphere on nearly all flights. For the most part, aerosols from different sources were well mixed, particularly in the boundary layer. For this reason, it is often difficult to extract the characteristics of each type. Moreover, the age of the air mass can be a major factor in their characteristics (e.g., larger particles will settle or be washed out). Median values of the lidar aerosol parameters for the aerosol types discussed are summarized in Table 1. The numbers in bold represent the median value in air masses most representative of that category without contributions from other categories. In the boundary layer, smoke and dust plumes were well mixed with anthropogenic aerosols and so some of these characteristics, particularly depolarization tend to be diluted. Therefore, boundary layer characteristics were selected only from cases with no depolarization and biomass burning characteristics were selected only above the boundary layer. As dust was only observed on two flights and most of it in the boundary layer, the

values shown do not represent the dust characteristics exclusively but rather an indication of the presence of dust.

Table 1. Characteristics observed in aerosol types.

	S_{IR}	S_{VS}	δ_{aer}	α
Stratospheric	< 0.5	< 0.15	--	> 2
Background	< 0.3	< 0.13	--	> 2.5
Polluted Free Troposphere	**0.51**	**0.14**	**0.38**	**1.78**
Boundary Layer	**3.6**	**0.3**	**0.5**	**0.49**
Biomass Burning	3 - 50	1 - 20	3 - 12	< 0.5
Dust	2.5 - 20	0.2 - 1	12 - 25	< 0.5
Aged Asian	0.5 - 1	0.2 - 0.5	< 1	1.5 - 2.5
Convective Outflow	0.5 - 5	0.2 - 1	< 1	1 - 2
Cirrus	> 100	> 5	> 40	< 0.5

3.1 Aerosol attenuation and extinction studies

The scattering ratios presented here and those that have been routinely computed from other field experiments have not been corrected for aerosol attenuation, which, depending on the aerosol type and the wavelength of the measurement, can be substantial. In order to provide quantitative information regarding aerosol attenuation, we have developed and implemented methodologies to retrieve profiles of aerosol extinction and optical thickness from these lidar data [5]. Algorithms have been developed using MODIS and aerosol model data to constrain the retrievals and early results show excellent comparisons with coincident measurements from remote sensing and in situ sensors [5, 6]. Fig. 4 shows the result of applying the aerosol attenuation correction to the scattering ratios derived from these retrievals. . These retrieval results will be used to further characterize the air masses observed during INTEX-NA.

4. ACKNOWLEDGEMENTS

All back trajectories and model results presented here are from the NOAA Aeronomy Lab / ICARTT analysis using the FLEXPART model.

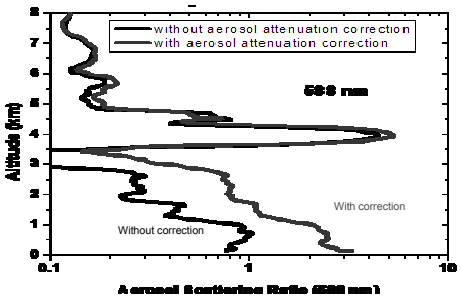

Fig. 4. Aerosol attenuation correction derived from MODIS constrained lidar retrievals.

We thank the entire team that contributed to the INTEX-NA field experiment, and in particular we want to acknowledge the contributions of Paul McClung, Lisa Hawks and Bill McCabe. The research reported here was funded by NASA's Tropospheric Chemistry and Radiation Science Programs.

5. REFERENCES

1. Browell E. V., Ismail S., and Grant W. B., Differential Absorption Lidar (DIAL) Measurements from Air and Space, *Appl. Phys. B*, *67*, 399-410, 1998

2. Browell E. V., et al., Large-scale air mass characteristics observed over the remote tropical Pacific Ocean during March-April 1999: Results from PEM-Tropics B field experiment, *J. Geophys. Res.,* **106***, 32,481-32,501*, 2001.

3. Jursa A. S., *Handbook of Geophysics and the Space Environment*, Air Force Geophysics Lab., U.S. Air Force, 1985.

4. Browell E. V., et al., Airborne Lidar Measurements of Ozone and Aerosol Distributions Over North America and the Western Atlantic Ocean During the INTEX-NA Field Experiment, 23rd ILRC (this issue).

5. Ferrare R. A., et al., Characterization of aerosols using airborne lidar and MODIS, MODIS Atmospheres, Meeting, Jan. 2006 (to be published in JGR) *http://modis.gsfc.nasa.gov/sci_team/meetings/200601 /presentations/atmos/ferrare.pdf?*

6. Ferrare R. A., et al., The Vertical Distribution of Aerosols: Lidar Measurements vs. Model Simulations 23rd ILRC (this issue).